A METHOD TO EVALUATE THE BENEFIT OF ENERGY-ABSORBING MATERIAL FOR SIDE IMPACT PROTECTION

David C. Viano
Biomedical Science Department
General Motors Research Laboratories
Warren, MI 48090-9055

Abstract

There are many opinions on the injury reducing benefit of energy-absorbing material for side impact protection. The objective of this study was to develop a methodology to link reductions in biomechanical responses due to force-limiting material to projections of injury mitigation in real-world side impact crashes, and to use this approach to evaluate the potential injury reducing benefit for the chest and abdomen of crushable material in the side door and armrest. Using a simulation of the human impact response, a range in crush force was determined which effectively reduced a peak biomechanical response from that obtained with a rigid impact. The range in constant crush force depended on the velocity of impact. The higher the velocity of impact, the higher the level of crush force to achieve a reduction in the peak response. NCSS field accident data for car-to-car side impacts provided information on the occupant exposure and injury as a function of the change in velocity (ΔV) of the struck vehicle. Based on various experimental studies, the velocity of the side door at contact with the occupant's chest is similar to the ΔV of the struck vehicle (about 60% of the closing speed of the striking vehicle). The chest impact velocity in the simulation was assumed equal to the observed ΔV in the NCSS data. This related the simulation data to real-world injury data. Reductions in biomechanical response were related to lower injury risk. This enabled a calculation of a reduction in injured occupants for the velocity range in which the EA material was effective. The greatest reduction in seriously injured occupants were found with relatively soft EA materials that are effective in the lower-speed (ΔV = 4 - 8 m/s) crashes, whereas padding was negligibly effective in high-speed crashes (ΔV > 10 m/s).

The Analytical Model

In 1973 Lobdell (1) published a lumped-mass model of the anteroposterior thoracic impact response of the human thorax. He postulated a mechanical analog of the human chest composed of two masses and connecting springs and dashpots; and, he matched the models force-deflection response to blunt impact data from human cadaver tests. The mechanical elements in the simulation (Figure 1) were adjusted until the model response fell within the low and high velocity force-thoracic deflection corridors recommended by Kroell (2) as representative of the human biomechanical response. Physically, elasticity is derived from the skeletal structures and the soft tissues and viscera within the chest. Damping is provided by air vented from the lungs, fluid moving through thoracic tissues and vessels and other energy dissipating mechanisms which are rate-dependent and dominate the biomechanical resistance of the chest for high velocities of impact.

The model was modified in this study to include a load-limiting interface on the impact mass and was validated by comparison with Hybrid III dummy experiments. It is useful for the evaluation of changes in biomechanical response with a range of load-limiting materials and severities of impact. Although this model is for frontal impact, it is one of the few analytical simulations of the chest that has been thoroughly studied in a wide range of applications and has stood the test of time within the biomechanics community. This model has been used as a representative simulation of the side impact response of the human thorax. Recent analyses of the force-deflection response of the human chest by Melvin (3) indicates that although the side impact thoracic response is slightly stiffer, the characteristic response and plateaus are very similar to that of the frontal impact response. Thus, the use of the modified Lobdell model seems to be appropriate until an equivalent lumped-mass simulation of the lateral thoracic impact response is available as a substitute in this analysis.

Lobdell's original lumped-mass model was modified by Viano (4) in 1978 to include the computation of kinetic energies, power, and momentum of the masses, and energy stored in springs and dissipated in dashpots during deformation of the chest. More recent modifications of the original Lobdell model include the feature of scaling size of the thorax from the 95th percentile male through the 5th percentile female to the six year old child. In this application, the model was further modified to include a thickness of force-limiting and energy-absorbing material between the rigid impactor and the lumped-mass thoracic model. The mechanical response of the thoracic model continues to possess four degrees of freedom, but the original equations of motion were modified if the impact force is sufficient to crush the interface material, if the full thickness of the material has been crushed, or if the impact force falls below that required to continue crushing the interface.

Figure 1 shows an example of the biomechanical responses obtained with the modified Lobdell model. The energy-absorbing interface crushes and limits force during a portion of the impact. In the example the full thickness of the energy-absorbing interface is crushed and there remains sufficient energy in the impact to increase the impact force after crush. With a crushable interface, there may be two impacts occurring during the simulation. The first is associated with the initial contact of the energy-absorbing interface with the chest and the response of the chest during crush of the energy-absorbing material. A second impact may occur when the full crush of the energy-absorbing interface occurs and there is sufficient energy to cause increases in the biomechanical responses of the chest. This second impact after full crush of the material can produce the greatest biomechanical responses in some cases and in others the maximum severity occurs during the first impact.

In this example, a 3.5 kN interface was selected with a 5 cm thickness. The impact severity is 10 m/s and the mass of the impactor is 20 kg. Force develops rapidly after contact with the chest and within several milliseconds is limited by crush of the energy-absorbing interface. Full crush of the interface occurs at 16 ms. After crush of the material, force on the chest increases and causes more chest deflection. The Viscous response (VC) of the chest is sensitive to the events occurring during impact. It rises to a peak during crush of the energy absorbing material and falls during mid-crush due to a reduction in the velocity of chest compression by interface crush. After full crush of the EA material, the relative velocity of chest compression

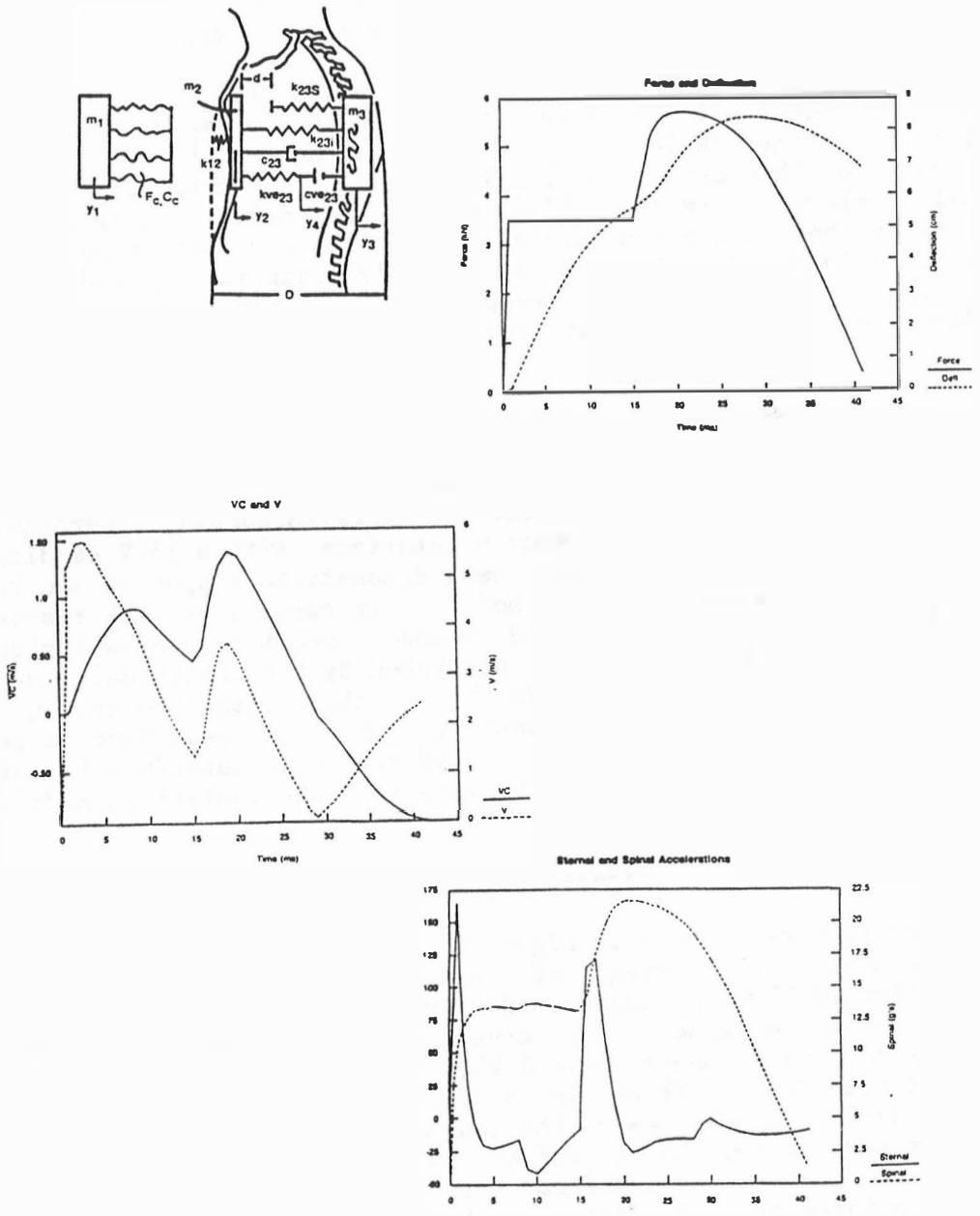

Figure 1: Lumped-Mass model of the chest and impacting mass with a load-limiting crushable interface (modified from (4)), and results of a simulation involving a 20 kg impactor striking the chest at 10.0 m/s with a 5 cm interface yielding at 3.5 kN.

increases and because of the higher levels of chest compression, the Viscous response reaches a maximum value during the second impact.

The acceleration of the sternum and spine demonstrate more of the dynamics of the chest response with an EA interface. In this example, the maximum sternal acceleration occurs during the initial contact with the EA material, just about the time that crush is initiated. During crush of the material, the sternal acceleration is controlled by the force-limiting interface until the material has bottomed and a second impact causes another spike. The second spike has a longer duration but is slightly lower in magnitude than the first peak. The spinal acceleration response is removed from the sternal dynamics and demonstrates a much smoother response.

Model Validation

The modified Lobdell model was validated by a series of chest impacts to the Hybrid III dummy. In these tests, an energy-absorbing interface was placed behind a light-weight (<.2 kg) wooden interface with a 15.2 cm diameter. The results from the Hybrid III dummy tests demonstrate responses and trends identical to those obtained with the model. In particular, the Viscous response in the dummy showed the first and second impact responses during and after crush of the EA interface just as predicted by the analytical simulation. In these tests at 6.7 m/s with a 23 kg impacting mass, the average difference between the predicted and experimentally obtained peak Viscous response was below 10% for the range of 1.8 - 4.6 kN crushable interface investigated and adds credence to the predictions obtained from the analytical model.

Parameter Study Conducted

The Viscous responses shown in Figure 2 for the 10 m/s impact severity and 5 cm thickness are for a range of constant crush-force EA interfaces. This superposition of Viscous responses demonstrates the shift in peak value from the first to second impact as the crush force of the material is reduced. For very stiff materials, those above 6 kN, the interface is so stiff that it acts as a rigid interface. There is no crush of the energy-absorbing interface occurring during impact because the contact force is below the crush force of 6 kN. However, as the EA interface is reduced in crush force, there is a reduction in Viscous response from crush and energy absorption by the interface. At a force of 4 kN, full crush of the interface occurs. If the crush force is further reduced in value, less energy is absorbed by crush of the interface and thus the greater remaining energy in the impactor causes an increase in the Viscous response. In this case, the increase in Viscous response is later in the impact and is associated with the after crush response. As the crush force is further reduced, the peak Viscous response increases until it reaches the level obtained with a rigid impact. The optimum Viscous response was obtained with a crush force that just completely uses the available crush space, and where the first and second peak are equal. In this case, the minimum value in Viscous response is obtained with a crush force of 4 kN.

Figure 3 summarizes the first and second peak values shown in Figure 2 and demonstrates the rigid impact response for crushable interfaces greater than 6

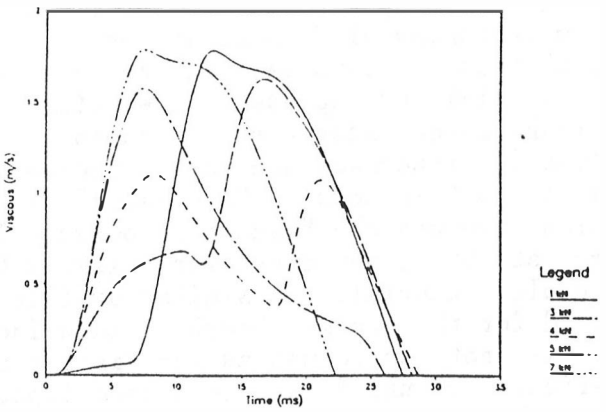

Figure 2: Superposition of Viscous responses with various crush force interfaces for a 10 m/s impact.

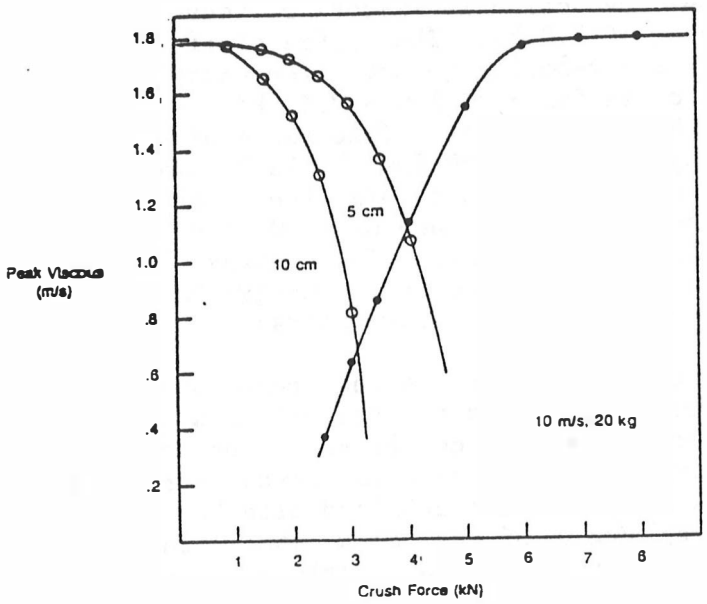

Figure 3: Peak Viscous responses with 5 cm and 10 cm of crushable interface showing the magnitude of the first peak during crush and second peak after crush in the Viscous response at 10 m/s.

kN crush force and the reduction in Viscous response with softer material. The minimum in Viscous response with 5 cm thickness of EA material occurs at 4 kN and results in a 40% reduction in peak Viscous response. The curve to the left that crosses and is marked as a 5 cm thickness represents the effects of second impact after crush with lower crush force materials. It shows an increase in Viscous response with a softening interface due to the increasing severity of the second impact. With a 10 cm thickness of EA material, there was a broader range of crush force which reduces the Viscous response. The increase in range of crush force occurs at the lower crush force levels because of the larger thickness of crushable material. A similar profile in reduction of chest compression was found for the energy-absorbing interface. However, the chest compression response is not as robust as the Viscous response and is less sensitive to the effects of the first and second impact. The insensitivity is, in part, due to the fact that chest compression is essentially the sum or overall effect of the entire impact loading.

Peak Viscous responses with a 5 cm thickness of EA material are plotted for four severities of impact in Figure 4 and demonstrate that the maximum realizable reductions in Viscous response are achieved at the lowest levels of impact severity. For the cases simulated here, a maximum of 70% was found for the 5 m/s impact at a crush force of 1.7 kN. In contrast, the maximum realizable reduction in Viscous response for the 12.2 m/s impact was 30% at a crush force of 5.2 kN. The range of effective energy-absorbing padding is narrower for low-velocity impacts (for example a 10% reduction is achieved in the range of crush force of 1.0 - 2.4 kN, which has a spread of 1.4 kN) than for the higher speed impacts (the range of effective EA interface is 3.8 - 6.4 kN with a spread of 2.6 kN for the 12.2 m/s impact). This curve also shows that for impact severities <7 m/s the peak Viscous response is below the currently recommended tolerance of 1.0 m/s (5) irrespective of choice of crushable interface material. In contrast, impact severities >10 m/s indicate that there is no choice for energy-absorbing interface that can reduce the peak Viscous response below tolerance.

It is possible to use the responses plotted in Figure 4 to define ranges of crush force which achieve either a 10% or 20% reduction in peak Viscous response for the 5 cm thickness of crushable interface. This type of analysis provides a range of crush force for which the peak Viscous response is below the maximum value obtained with the rigid interface by >10% or >20% and allows a replotting of the data where the severity of impact is the controlling parameter. Figure 5 provides a summary of the crush-force corridors which reduce the peak Viscous response as a function of the severity of impact. For a given velocity of impact or severity, the upper limit is defined as the maximum crush force achieving either a 10% or 20% reduction of peak Viscous response. Selecting a crush force that is greater gives a material that is too rigid to produce at least a 10% reduction in Viscous response. The lower limit at each severity of impact is controlled by the thickness of the crushable material and minimum crush force to achieve a 10% reduction in Viscous response. Selection of a softer material can provide effective reductions in peak Viscous response only if it is thicker such as is demonstrated by the lower crush force corridor for the 10 cm thickness material. This graph includes regions in which padding can reduce the Viscous response below the accepted tolerance level. The region is much smaller than that producing reduction in the Viscous response irrespective of magnitude. All impacts below 7 m/s result in a peak Viscous response that is below tolerance.

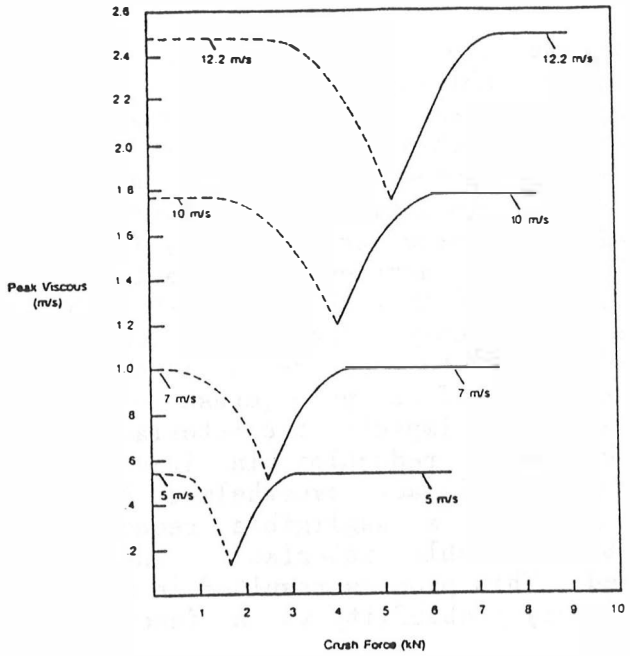

Figure 4: Peak Viscous response during crush of various interfaces at four severities of impact.

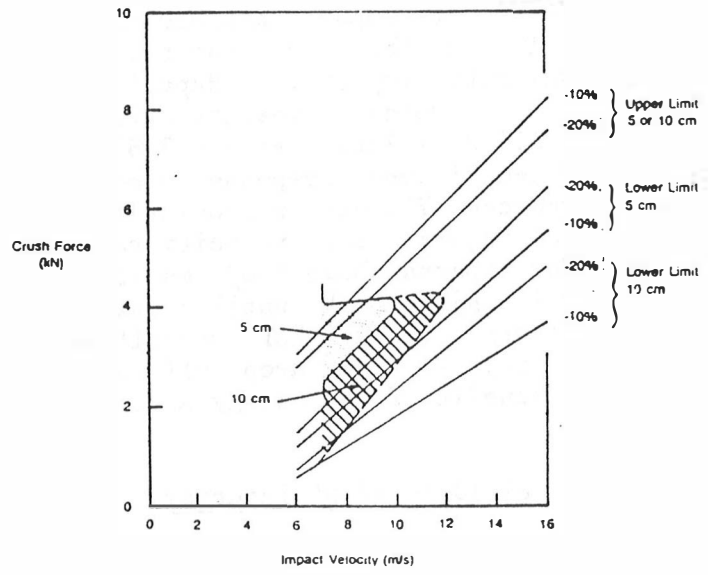

Figure 5: Corridors of >10% and >20% reduction in peak Viscous response for a 5 cm or 10 cm thickness crushable interface. Overlayed with regions in which the Viscous response may be kept below tolerance with padding.

Injury Reducing Effects of Padding

The method employed to evaluate injury reductions associated with an EA interface used the injury probability function (Figure 6) for AIS ≥3 injury directly with the response data obtained for rigid impacts (baseline injury probability), and responses with a crushable interface. The approach does not consider whether the peak Viscous response is associated with the first or second impacts and requires simulations at a larger number of severities of impact. Velocities of impact were incremented by 1 m/s from a low of 1 m/s to a high of 18 m/s. For each increment in impact severity, the peak Viscous response for a rigid impact and that obtained with a thickness of a particular interface crush force was directly related to a probability of AIS ≥3 injury. It was then straight-forward, to compute a percent reduction in the probability of injury for each interface pair (crush force or stiffness and thickness). For very low severity impacts the interface crush force could be too high to crush and achieve a reduction in injury probability. For high severity impacts either the impact overwhelmed the response or the injury probability was so high that a negligible reduction in injury probability could be produced by the crushable interface. In the mid-region, injury reduction may be realized. This process resulted in a relationship defining the percent reduction in injury probability as a function of the severity of impact and EA interface.

Figure 7 shows the peak Viscous response as a function of impact velocity with a rigid interface and with two constant crush force pads of 5 cm or 10 cm thickness and crush force of 3.5 kN and 6.25 kN. For the 3.5 kN constant crush force interface, the energy absorbing pad reduces the peak Viscous response for impacts of greater than 6 m/s velocity. The reductions in Viscous response are limited to an interval of impact velocity as the 5 cm curve approaches the rigid response for severities of impact approaching 12 m/s. The range of benefit is larger for the 10 cm thickness pad but also approaches the rigid response for the higher severity impacts. Superimposed on this curve is a line just above VC = 2.0 m/s which represents a Viscous response associated with a 99% probability of AIS 3+ injury. With a 3.5 kN crush force interface, the velocity range of reduced Viscous response is below the 99% injury probability level. When the reduced Viscous responses are converted to a percent reduction in probability of injury, the velocity range of benefit is clearly identified (Figure 8). For impacts above 6 m/s severity, there is a continual increase in the reduction in injury risk until a maximum value is obtained at a level approaching 65% lower risk. For severities of impacts above that level, the reductions in injury risk drop off until a severity level is reached where there is no benefit of the energy absorbing interface.

Field Accident Injuries

The NCSS field accident data for car-to-car side impacts was analyzed (6) to determine occupant exposures and injury risks as a function of the computed change in velocity (ΔV) of the struck vehicle. The injury risk function (the probability of injury as a function of the change in velocity of the struck vehicle) was computed from the available information on the number of occupants exposed and the number injured of severity AIS 3+ for each 1.35 m/s (3 mph) increment of ΔV. This resulted in 15 increments in ΔV for the field accident data covering the full range of crashes observed in real-world side

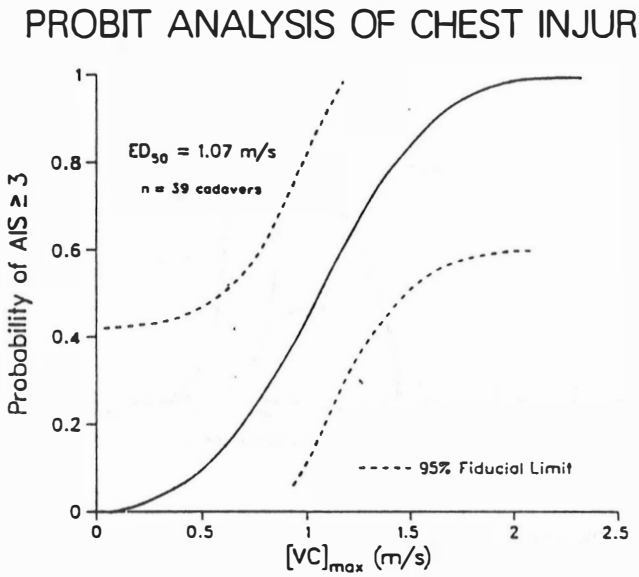

Figure 6: Chest injury risk function relating the probability of AIS 3+ injury as a function of the peak Viscous response (derived from (5)).

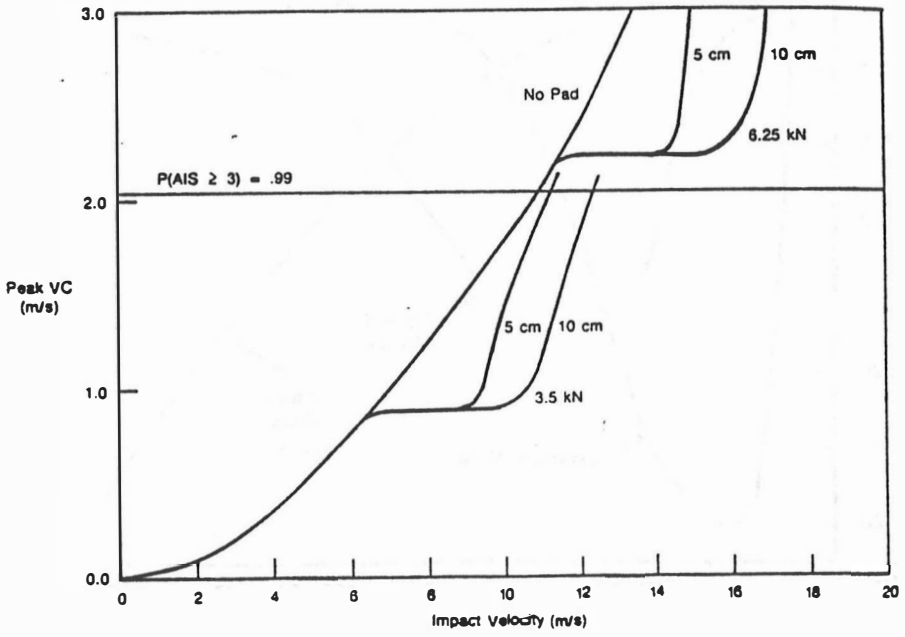

Figure 7: Demonstration of the reductions in peak Viscous response with a 5 or 10 cm thickness of constant crush force interfaces of 3.5 or 6.25 kN crush force, and the range of benefit in reduced peak Viscous response in relation to the 99% injury probability line for AIS 3+ trauma.

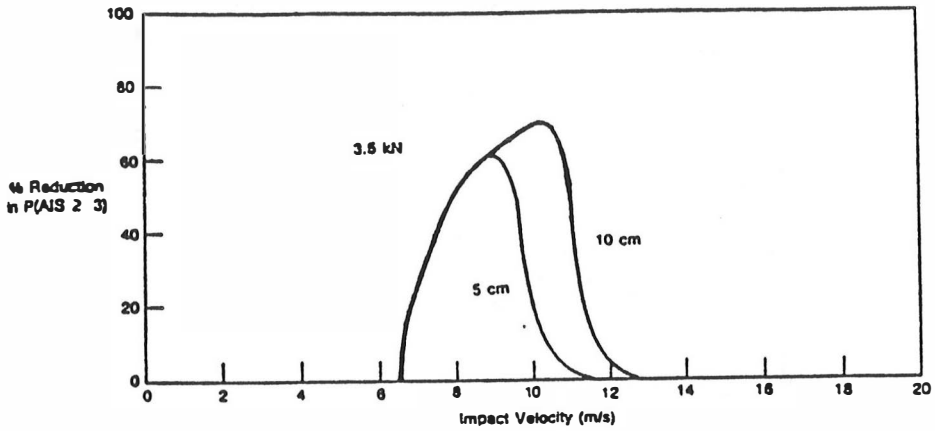

Figure 8: Percent reduction and probability of AIS 3+ injury for a 3.5 kN constant crush force interface of 5 cm or 10 cm thickness (note that a comparable curve could not be drawn for a 6.25 kN crush force interface since its projected reductions in AIS 3+ injury risk were zero over the range of impact severities.)

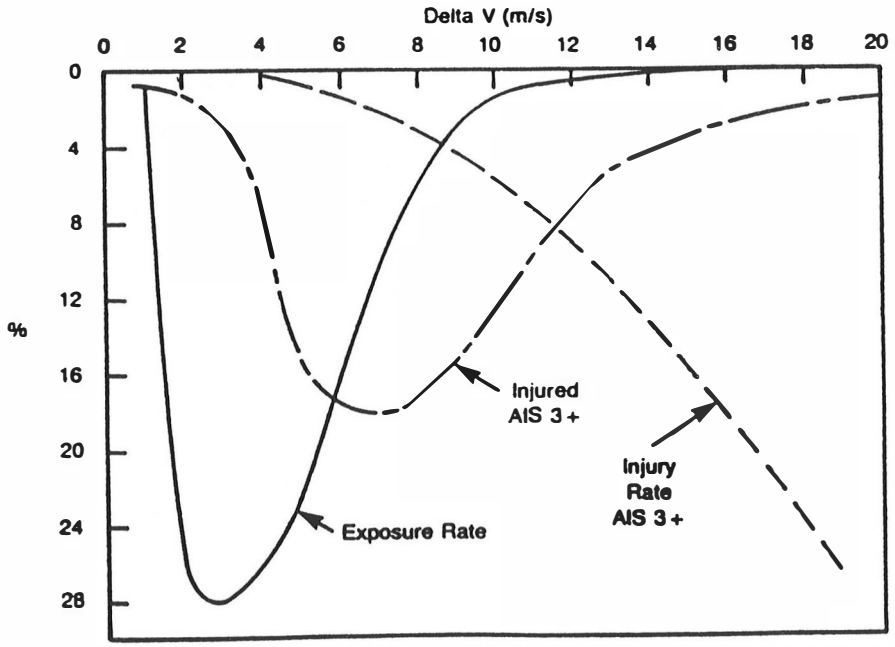

Figure 9: Distribution of occupants exposed and injured AIS 3+ in car-to-car side impacts, and the risk of injury as a function of the ΔV of the struck vehicle (derived from NCSS (6)).

impacts (Table 1). In addition to the raw data on the actual number of occupants exposed and injured occupants, exposure rates and injury rates are computed based on the total sample of exposed occupants (30,084) and seriously injured occupants (396). Figure 9 shows the pattern of exposure and injured occupants as a fraction of the total number of exposed and injured people. The maximum exposure occurs at the lower speeds of impact, between 1.5-6.2 m/s. Because the injury rate increases with the severity of the side impact, the peak in injuries is shifted to a higher crash severity. The peak in injured occupants occurs at 7 m/s. As might be expected, the maximum injury rate occurs for the highest severity crashes and peaks at about 30% risk based on smoothed curves of AIS 3+ for a 20 m/s ΔV crash.

Linking Laboratory Tests to Real-World Crashes

It was possible to link the range of reduced thoracic responses obtained with energy-absorbing material to the real-world field accident injury data by relating the ΔV of the struck vehicle in the NCSS data to the velocity of impact in the simulation. The French published data (7) on car-to-car side impacts, where the deformation characteristics of the struck vehicle were measured. These 14 m/s (30 mph) side impacts demonstrated (Table 2) that the ΔV of the struck vehicle closely approximates the maximum (intrusion) velocity of the side door. This data provides the link between the simulation and real-world accidents, and indicates a one-to-one correspondence between impact velocity in the simulation and ΔV from field accident data.

Injury Reductions with Padding

A reduction in injured occupants was computed by lowering the value of injury risk in the NCSS data for the range of velocities where the EA material provides benefit. By reducing the injury risk in the effective range of the padding, the lower value of injury risk was multiplied by the actual number of exposed occupants to compute a new, but reduced, number of injured occupants. The difference between the actual number injured and the reduced injured represents a savings in injured people for a particular 1.35 m/s increment of ΔV. The reduced number of injured occupants for each velocity corridor was divided by the total number of injured in the original NCSS data set to obtain a fraction of injury reduction for that corridor. Summing the injury reducing fractions over the effective velocity range of the energy-absorbing material gave a projection for the overall benefit (reduction in AIS 3+ injuries) for a particular thickness and crush force of an interface material.

Using Figure 8 and the actual real-world side impact injury data from the NCSS analysis, it is possible to project a 15.3% reduction in injured occupants with a 5 cm thick pad of 3.5 kN crush force (Table 3). There is a slight increase in projected benefit with a 10 cm thick pad. For a constant crush force interface of 6.25 kN stiffness, Figure 7 showed that the range of reduced peak Viscous response is at the higher severity impacts (approximately 12-16 m/s impact) and that this range is well above the 99% injury risk level. When a curve similar to Figure 8 was attempted, the reduction in Viscous response for these severe impacts did not produce a reduction in injury risk. A pad of this crush force would be projected to have no benefit in reducing real-world occupant injuries primarily because its range of effectiveness is

Table 1

CAR-CAR SIDE IMPACT CRASHES AND INJURIES FROM NCSS ACCIDENTS

Mean Delta V	Occupant Exposure		Injured AIS 3+	
	Number	Rate	Number	Rate
m/s		%		%
1.35	1722	5.72	3	0.17
2.70	7407	24.62	10	0.14
4.05	7938	26.39	28	0.35
5.40	6114	20.32	70	1.14
6.75	3042	10.11	62	2.04
8.10	1965	6.53	77	3.92
9.45	693	2.30	33	4.76
10.80	372	1.24	11	2.96
12.15	387	1.29	24	6.20
13.56	285	0.95	36	12.63
14.85	75	0.25	22	29.33
16.20	45	0.15	5	11.11
17.55	21	0.07	3	14.29
18.90	18	0.06	12	66.67
20.25	0	0.0	0	0.0
Totals	30084		396	

Table 2

CAR-CAR SIDE IMPACTS

Impact Speed	13.92 * .28 m/s
Delta V (Struck Vehicle)	8.28 * .92 m/s
Delta V (B-Pillar)	8.03 * .94 m/s
Maximum Door Velocity	8.56 * 1.40 m/s

Table 3

BENEFITS OF ENERGY-ABSORBING PADDING IN SIDE IMPACT PROTECTION

Constant Crush	5 cm	10 cm
6.25 kN	0.00(0.0)	0.00(0.00)
3.50 kN	15.32(1.84)	18.58(2.23)

* First number is percent reduction in AIS 3+ injuries in side impacts and in parentheses the percent reduction in total harm.

in such severe impacts that the injury probabilities are well above 99% and are not effected by the reductions in Viscous response.

Malliaris (8) studied total occupant Harm in automobile crashes and found that 12% of total Harm is related to side interior and arm rest contacts. Since these are the surfaces where EA and force-limiting material could influence injuries in side impact crashes, the maximum Harm reduction with the introduction of padding must be less than 12%. In fact, the overall reduction in total Harm achieved by padding is the product of the projected reductions in injured occupants and the fraction of Harm due to side interior and armrest contact (in this case even if the padding were 100% effective, it would result in only a 12% reduction in total Harm). Table 3 shows the overall reduction in Harm achievable by energy-absorbing padding with a crush force of 6.25 kN or 3.50 kN. With 5 cm thickness of the 3.5 kN crush-force material, the 15.3% reduction in total injured relates to a 1.8% reduction in total crash injury Harm. Note that there is no projected reduction in injuries and Harm with an EA interface having a 6.25 kN crush force.

Discussion

The results of this study show that beneficial reductions in occupant injury may be realized with the appropriate selection of an energy absorbing material. By shifting from materials that are effective in the most severe accident exposures to softer materials that work in the range where the greatest number of severe injuries are occurring (the lower severity accident exposures), reductions in the range of 15% - 20% in AIS 3+ injuries may be possible with EA material thicknesses of 5 cm - 10 cm. The results of this analysis are encouraging and indicate potential gains in occupant protection and Harm reduction by side impact padding. However, this study should be considered a first step in the development of a more refined procedure for the selection of engineering requirements for occupant safety systems.

Obviously the ultimate goal of this type of analysis is the eventual formulation of a scientific basis for safety engineering which recognizes the wide range of crash severities in which occupants are injured, provides assurance that safety measures are effective over the greatest range of crash exposures, and involves impact testing and evaluations that focus on crashes where the greatest number of injuries are occurring, rather than focusing on selected high-severity crash exposure. This is particularly important since the results of this study indicate that optimization of EA material interfaces in high-severity crash exposures may lead to the selection of materials that have a negligible effect on improving occupant protection (see particularly the projected benefits of a high constant crush force material which might be identified as the optimum to reduce a biomechanical response from a dummy test but which on the basis of this analysis would be projected to have no benefit in reducing real-world occupant injuries). Hopefully, this type of analysis is the first of a series of efforts to develop and refine a scientific basis for safety engineering which ultimately will result in effective engineering practices for the reduction of real-world injury and Harm, and for injury control.

This analysis concludes that paddings should be matched to crashes where the greatest number of injuries are occurring in real-world accidents. It points particularly to the risks of selecting tests that are of very high severity

even though they indicate a significant reduction in biomechanical response from either a simulation or dummy test. Since the goal is the eventual reduction in real-world injuries, the results of this type of analysis may be helpful in the ultimate selection of test parameters for a full-scale side impact test.

The study has not focused on the comparable benefits that might be realized by other types of energy-absorbing interface or structural-vehicle modifications. Structural changes may reduce the effective contact velocity or severity of impact on the occupant. The inclusion of the later type or benefit analysis may be useful prior to any ultimate evaluation of the effectiveness of a particular countermeasure in side impact protection. However, this analysis does offer promise to the safety benefits of impact padding when the material and its characteristics are optimized in crashes where the greatest numbers of injuries are occurring, and where the padding is effective in reducing injury risk on the steepest portion of the sigmoidal response (clearly not in the areas of the asymptotic response at 100% probability or zero probability of injury), and where all the factors of crash injury protection are considered in the context of the wide diversity of real-world accidents.

References

1. Lobdell, T.F., "Impact Response of the Human Thorax." Proceedings of the Symposium Human Impact Response Measurement and Simulation, General Motors Research Laboratories, Oct. 2-3, 1972, New York-London: Plenum Press, pp. 201-245, 1973.

2. Kroell, C.K., "Thoracic Response to Blunt Frontal Loading." In The Human Thorax-Anatomy, Injury and Biomechanics, P-67, Society of Automotive Engineers, Inc., pp. 49-78, 1976.

3. Melvin, J.W., King, A.I., and Alem, N.M., "AATD System Technical Characteristics, Design Concepts, and Trauma Assessment Criteria," The University of Michigan, Department of Mechanical Engineering and Applied Mechanics Contract No. DTNH22-83-C-07005, Task E-F, Final Report, September, 1985.

4. Viano, D.C., "Evaluation of Biomechanical Response and Potential Injury from Thoracic Impact." J of Aviat. Space and Environ. Med. 49(1):125-135, 1978.

5. Viano, D.C., and Lau, I.V., "Thoracic Impact: A Viscous Tolerance Criterion," 1985 NHTSA Symposium on Experimental Safety Vehicles, Oxford, England, June 1985.

6. Rouhana, S.W., and Foster, M.E., "Lateral Impact - An Analysis of the Statistics in the NCSS." Society of Automotive Engineers Technical Paper No. 851727, 1985.

7. Dargaud R., and Bourdillon, T., "Simulation of Lateral Impact with Mobile Deformable Barrier." Society of Automotive Engineers Technical Paper No. 860051, 1986.

8. Malliaris, A.C., Hitchcock, R., and Hedlund, J., "A Search for Priorities in Crash Protection." Society of Automotive Engineers Technical Paper No. 820242, 1982.